CROATICA CHEMICA ACTA
CCACAA, ISSN 0011-1643, e-ISSN 1334-417X
Croat. Chem. Acta **84** (1) (2011) 39–52.
CCA-3448

Original Scientific Article

An Analytical Approach for Calculating Transfer Integrals in Superexchange Coupled Dimers

Stefan Lebernegg,* Georg Amthauer, and Michael Grodzicki

Department of Materials Engineering and Physics, University of Salzburg, Hellbrunnerstrasse 34, 5020 Salzburg, Austria

RECEIVED SEPTEMBER 29, 2010; REVISED DECEMBER 20, 2010; ACCEPTED DECEMBER 22, 2010

Abstract. An analytical expression for the transfer integral H_{AB} between the localized magnetic orbitals in superexchange-coupled dimers as a function of the type of atoms and geometry of the molecule has been derived by explicitly including orbital interactions. It is shown that H_{AB} plays the key role for understanding magneto-structural correlations. The reliability and capability of this approach is confirmed by comparison with numerical electronic structure calculations in the local spin-density approximation on singly and doubly bridged Cu(II)-dimers with fluorine ligands. All results can be calculated and understood within the analytical formalism representing, therefore, a powerful tool for understanding the magneto-structural correlations and for constructing magnetic orbitals analytically. (doi: 10.5562/cca1760)

Keywords: molecular magnetism, superexchange, model Hamiltonian, density functional theory

I. INTRODUCTION

The isotropic magnetic interaction between localized spins at centers A and B may be described by the Heisenberg-Dirac-van Vleck Hamiltonian

$$H = -2J \cdot \hat{S}^A \hat{S}^B \tag{1}$$

where the (isotropic) Heisenberg coupling constant J describes the strength and mode of the magnetic coupling. With regard to the sign convention in Eq. (1) J is positive for parallel or ferromagnetic coupling and negative for antiparallel or antiferromagnetic alignment of the two spins. Besides the quantitative determination of the size and sign of J in particular systems, the central purpose of a general theory of superexchange is to identify and to deduce the various geometric and electronic factors responsible for the mode of interaction between the spins in exchange coupled systems.[1] The various attempts of determining J can roughly be described as follows:

(i) Experimentally, J can be derived from spectroscopic data as EPR spectra[2] or from temperature dependent magnetic susceptibility measurements.[3] On this level nothing can conclusively be said about the nature and origin of the magnetic interactions determining sign and size of J.

(ii) Phenomenologically, a number of empirical rules and correlations have been inferred from the observation of certain regularities. Examples are the Goodenough-Kanamori rules[1,2] interpreted later by Andersons theory of superexchange[6] or the frequently proposed exponential dependence of J on the distance between the interacting magnetic centers.

(iii) Theoretically, J can be determined by numerical electronic structure calculations, especially by methods based on density functional theory (DFT)[7] in combination with the broken symmetry formalism.[8] Even though the dependence of J on certain parameters can be investigated by systematic numerical model calculations, it is almost impossible to derive manageable analytical expressions for understanding magneto-structural correlations on that high level of sophistication.

Accordingly, none of these three approaches enables the derivation of explicit formulas for J as a function of geometrical parameters, electronic properties of the metal centers, nature of the bridging and terminal ligands *etc*. Moreover, both the size of the experimentally investigated real systems and the complex nature of the magnetic interactions in those systems make it difficult to establish an explicit connection between the molecular (geometric and electronic) structure and magnetic properties by deriving an analytical expression for J, and a systematic analysis of the dependence of J on these factors has not yet been reported to the best of our knowledge. It is, thus, necessary to select

* Author to whom correspondence should be addressed. (E-mail: stefan.lebernegg@sbg.ac.at)

model systems that are simple enough to allow an approximately analytical treatment but, at the same time, are close enough to real systems where experimental data are available for comparison. Such paradigmatic model systems are binuclear Cu(II) complexes with halogens, oxygen or OH groups as bridging ligands since they contain a single magnetic orbital per metal center and exhibit antiferromagnetic as well as ferromagnetic coupling depending on the nature and arrangement of the bridging and the terminal ligands.[1,9] Moreover, such systems are of great practical importance due to their occurrence in biological systems[10] and in high-T_c superconductors.[11]

For a dimer with one magnetic orbital per metal centre, as realized in Cu(II)-dimers, the coupling constant for superexchange may be approximated by:[6,12]

$$J = K_{AB} - \frac{2\left(H_{AB}\right)^2}{U_{AA} - U_{AB}} \tag{2}$$

where the two-electron exchange integral K_{AB} is always positive, hence leading to ferromagnetic coupling. The second term represents the antiferromagnetic contribution and arises from the (weak) delocalization of the magnetic orbitals towards the bridging ligands.[6] Extensions of this first approximation have been discussed[13,14] and thoroughly been reviewed[15] but for systems with a single nondegenerate magnetic orbital per metal Eq. (2) is known to be sufficiently accurate. Another class of problems arises when using Eqs. (1,2) in combination with numerical calculations within the frame of density functional theory (DFT). The first one concerns the proper definition of localized spins entering the Heisenberg Hamiltonian, Eq. (1). The various possibilities for such a definition have recently been discussed[16,17] and reviewed.[18] However, the investigations of this work aiming at deriving qualitative magneto-structural correlations do not depend on such definitions. The second kind of problems concerns the direct numerical calculation of J by DFT methods since Eq. (2) originates from a configuration interaction (CI) analysis[12] and DFT and CI calculations consider the electron correlation in different ways. However, based on a spin polarization perturbation orbital theory Seo[19] pointed out that the structure of Eq. (2) is preserved for localized MO's derived from a DFT calculation.

Among the various integrals occurring in Eq. (2) both the ferromagnetic term and the denominator, *i.e.* the effective on-site electronic repulsion $U = U_{AA} - U_{AB}$, of the second term are expected to vary only slightly with geometry.[20] By contrast, the transfer integral H_{AB} that is roughly a function of the overlap integral between the magnetic orbitals of the parent monomers forming the molecule or solid[21,22] strongly depends on geometry. Correspondingly, H_{AB} *is* the key parameter for deriving and understanding magneto-structural correlations. Although the transfer integral may be obtained from numerical electronic structure calculations, the analysis of the various contributions to H_{AB}, as well as the extraction of those interactions dominating the magneto-structural correlations are usually complicated if possible at all, *i.e.* the detailed structure of the magnetic coupling mechanism remains hidden. Accordingly, this work aims at deriving an expression for H_{AB} and J which has a sound physical basis in the sense that its general functional form can be justified by theoretical reasoning while the system-dependent parameters have a well defined physical meaning insofar as they can be determined, at least in principle, from sufficiently accurate numerical calculations. Although the derivation is carried out for homonuclear transition metal dimers with a single unpaired electron per metal centre, the final result will be applicable, as well, to heteronuclear complexes with more than one unpaired electron per metal site. For the latter case a generalized expression of Eq. (2) has to be used (see *e.g.* Ref. [23]).

After some basic definitions of magnetic orbitals and transfer integrals in the second section, different approaches for their analytical calculation are derived in section three, and will be applied on several Cu-F model systems in section four. In the last section the correlation between the transfer integral and J is investigated in detail and an analytical expression for J will be used for estimating the magnetic behavior of the model complexes. Finally, the analytical transfer integrals and coupling constants will be compared with the results of two different numerical DFT-codes.

II. GENERAL BASIS

In the CI analysis from which Eq. (2) is derived the transfer integral H_{AB} is defined as[23]

$$H_{AB} = \left\langle \psi_A \middle| H \middle| \psi_B \right\rangle = \left\langle \psi_A(1) \middle| h(1) \middle| \psi_B(1) \right\rangle + \left\langle \psi_A(1)\psi_B(2) \middle| |r_{12}|^{-1} \middle| \psi_B(1)\psi_B(2) \right\rangle \tag{3}$$

where H is the Fock-operator. $h(1)$ is the one-electron Hamiltonian and ψ_A and ψ_B are the magnetic, *i.e.* singly occupied molecular orbitals (MO's) of the dimer localized on the metal centers A and B, respectively. These orbitals contain the active electrons. The two-electron (bondcharge) integral is generally regarded as negligible.[12,8,24] As already mentioned Seo[19] pointed out that the structure of Eq. (2) is preserved for localized MO's derived from a DFT calculation where the transfer integral is defined as the expectation value of a spin-restricted DFT-Hamiltonian with energy-localized molecular orbitals containing the active electrons. These localized MO's are constructed by linearly combining

the delocalized highest occupied (HOMO) and the lowest unoccupied (LUMO) Kohn-Sham orbitals of the dimer, denoted as ψ_+ and ψ_-,

$$\begin{aligned}|\psi_A\rangle &= \cos\gamma\cdot|\psi_-\rangle + \sin\gamma\cdot|\psi_+\rangle \\ |\psi_B\rangle &= -\sin\gamma\cdot|\psi_-\rangle + \cos\gamma\cdot|\psi_+\rangle\end{aligned} \tag{4}$$

where γ has to be estimated numerically in order to maximally localize the orbitals. For symmetric dimers Eq. (4) reduces to

$$\begin{aligned}|\psi_A\rangle &= 2^{-1/2}|\psi_+ + \psi_-\rangle \\ |\psi_B\rangle &= 2^{-1/2}|\psi_+ - \psi_-\rangle\end{aligned} \tag{5}$$

Accordingly, the transfer integral is given as

$$\begin{aligned}H_{AB} &= \langle\psi_A|H|\psi_B\rangle \\ &= \frac{1}{2}\langle\psi_+ + \psi_-|H|\psi_+ - \psi_-\rangle = \frac{1}{2}(\varepsilon_+ - \varepsilon_-)\end{aligned} \tag{6}$$

where ε_+ and ε_- are the orbital energies of ψ_+ and ψ_-. For symmetrical, planar, doubly bridged transition metal (TM)-dimer these orbitals are depicted in Figure 1 B,C).

The aim is to construct localized dimer MO's, $|\psi_A\rangle$ and $|\psi_B\rangle$, in such a way that an analytical expression for the transfer integral and correspondingly for the coupling constant *J* can be derived. To this end, Anderson[6] suggested, in a first step, to solve the parent monomer problems, *i.e.* to construct the singly occupied MO of each of the two monomers (Figure 1A), which, in a second step, are linearly combined to give the HOMO and LUMO of the dimer.

$$\begin{aligned}|\psi_\pm\rangle &= N_\pm\left(|\psi_A^{\text{mono}}\rangle \pm |\psi_B^{\text{mono}}\rangle\right) \\ &= 2^{-0.5}\left(1 \pm S_{AB}^{\text{mono}}\right)^{-0.5}\left(|\psi_A^{\text{mono}}\rangle \pm |\psi_B^{\text{mono}}\rangle\right)\end{aligned} \tag{7}$$

with the overlap matrix element $S_{AB}^{\text{mono}} = \langle\psi_A^{\text{mono}}|\psi_B^{\text{mono}}\rangle$. Combining the delocalized orbitals $|\psi_+\rangle$, $|\psi_-\rangle$, Eqs. (4) or (5), gives the localized singly occupied dimer MO's $|\psi_A\rangle$, $|\psi_B\rangle$. H_{AB} may then be expressed in terms of the monomer orbitals, where $\varepsilon_{A,B}^{\text{mono}} = \langle\psi_{A,B}^{\text{mono}}|H|\psi_{A,B}^{\text{mono}}\rangle$:

$$H_{AB} = \frac{1}{2}\begin{pmatrix}\varepsilon_A^{\text{mono}}\left(N_+^2 - N_-^2\right) + \varepsilon_B^{\text{mono}}\left(N_+^2 - N_-^2\right) + \\ 2\langle\psi_A^{\text{mono}}|H|\psi_B^{\text{mono}}\rangle\left(N_+^2 + N_-^2\right)\end{pmatrix} \tag{8}$$

Assuming S_{AB}^{mono} to be small the normalization factors can be approximated up to first order by $N_\pm^2 = \frac{1}{2}\left(1 \mp S_{AB}^{\text{mono}}\right)$ so that for a symmetric dimer Eq. (8) simplifies to

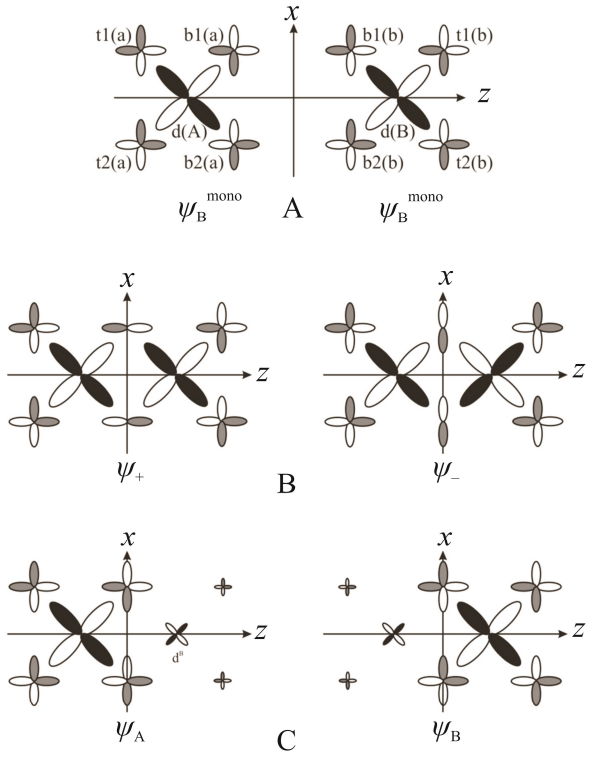

Figure 1. Construction of localized MO's of a planar, symmetrical, doubly bridged dimer placed in the *xz*-plane. d(*X*) is a transition metal d-orbital on monomer centre *X*. t1(*x*), t2(*x*), b1(*x*) and b2(*x*) are the p_z- and p_x-orbitals of the terminal (t) and bridging (b) ligands, respectively, on centre *x* (for ligand orbitals the centre is written in lower case). The shadings indicate the phases of the wave functions and exhibit the antibonding character of the MO's ψ_X^{mono}. The ligand s-orbitals are omitted. The size of the orbitals is proportional to their contribution to the respective MO. A: Decomposition of the dimer into two monomers and construction of the two singly occupied monomer MO's. In contrast to the p_z-orbitals, the p_x-orbitals of the bridging ligands of the two monomers have different phases. B: The delocalized HOMO and LUMO of the dimer; C: The localized singly occupied MO's.

$$H_{AB} = -\varepsilon^{\text{mono}}\cdot S_{AB}^{\text{mono}} + H_{AB}^{\text{mono}} \tag{9}$$

where $\varepsilon^{\text{mono}} = \varepsilon_A^{\text{mono}} = \varepsilon_B^{\text{mono}} = \langle\psi_B^{\text{mono}}|H|\psi_B^{\text{mono}}\rangle$ and $H_{AB}^{\text{mono}} = \langle\psi_A^{\text{mono}}|H|\psi_B^{\text{mono}}\rangle$.

Alternatively, Löwdin orthogonalization of the monomer MO's yields localized orbitals, as well:

$$|\psi_A\rangle = N_A\left(|\psi_A^{\text{mono}}\rangle - \frac{1}{2}S_{AB}^{\text{mono}}|\psi_B^{\text{mono}}\rangle\right) \tag{10}$$

with an analogous expression for $|\psi_B\rangle$ and the normali-

zation factor $N_A = \left(1 - \frac{3}{4}\left(S_{AB}^{\text{mono}}\right)^2\right)^{-0.5}$. This construction should be more suitable for nonsymmetrical dimers since it circumvents the problem of numerically estimating γ in Eq. (4). With Eq. (10) the transfer integral may be written as

$$H_{AB} = N_A \cdot N_B \cdot \begin{pmatrix} H_{AB}^{\text{mono}} - \frac{1}{2} S_{AB}^{\text{mono}} \cdot \varepsilon_A^{\text{mono}} \\ -\frac{1}{2} S_{AB}^{\text{mono}} \cdot \varepsilon_B^{\text{mono}} \end{pmatrix} \qquad (11)$$

if the small term proportional to $\left(S_{AB}^{\text{mono}}\right)^2$ is neglected. For the special case of a symmetric dimer Eq. (11) reduces to Eq. (9) to first order in S_{AB}^{mono}. In deriving an analytical expressions for the transfer integral the monomer approach will be discussed first. Since in some cases the analytical solution of the monomer problem is impossible with sufficient accuracy, alternatively the dimer-MO's $|\psi_+\rangle$ and $|\psi_-\rangle$ will be directly constructed in order to arrive at analytical expressions for the transfer integral.

These different procedures for calculating H_{AB} will be discussed in detail for doubly bridged $[Cu_2X_2Y_4]^{n-}$ dimers. Afterwards the analytical approaches will be applied to simple model complexes and the results will be compared with fully numerical calculations. Finally, the analytical transfer integrals will be utilized for reproducing and understanding the numerically calculated coupling constants of these complexes.

III. CALCULATION OF H_{AB}

A. Monomer Approach

As already pointed out, the basic problem in analytically calculating H_{AB} consists in the construction of appropriate singly occupied monomer MO's, Eq. (7), exhibiting predominantly transition metal d-character. An analytical approach for constructing such orbitals has already been described[25] and proven to be sufficiently accurate for describing d-orbital splitting patterns of TM-complexes.[26] This analytical approach transforms the full multi-centre MO-Hamiltonian of a TM surrounded by *N* ligands into a single-centre problem in two steps: in the first step the Kohn-Sham equation is solved in linear combination of atomic orbital (LCAO) approximation with respect to metal atomic d-orbitals that are Schmidt-orthogonalized to the ligand atomic orbitals (AO's):

$$\left|\tilde{\varphi}_{\text{d}}^X\right\rangle = N_{\text{d}}^X \left(\left|\varphi_{\text{d}}^X\right\rangle - \sum_i S_{\text{d}i}^{Xx} \left|\varphi_i^x\right\rangle \right) \qquad (12)$$

where $S_{\text{d}i}^{Xx}$ is the overlap matrix element between a metal d-orbital on centre *X*, $\left|\varphi_{\text{d}}^X\right\rangle$, and ligand AO *i*, $\left|\varphi_i^x\right\rangle$, on centre *x* and $N_{\text{d}}^X = \left(1 - \sum_i S_{i\text{d}}^{xX}\right)^{-1/2}$ is the normalization factor. The sum runs over all ligand AO's which are assumed to be orthogonal to each other. In order to simplify the procedure the ligand AO's are combined linearly to obtain symmetry adapted group-orbitals corresponding to the symmetry of the singly occupied monomer MO. The summation in Eq. (12) is then restricted to these group-orbitals. In the subsequent discussions ligand orbitals are always understood as group-orbitals, if not mentioned otherwise. Each AO is described by the product of a single Slater-type orbital (STO) and a real spherical harmonic, where the orbital exponent has turned out to be rather insensitive to geometrical changes of the dimers and is therefore taken as constant. In the second step, the Hamiltonian matrix calculated with the orthogonalized ligand and metal orbitals is diagonalized by a nondegenerate second-order perturbation calculation, *i.e.* the contribution of the nondiagonal elements to the energy of the ligand-orthogonalized d-orbital is accounted for in second order. If nondiagonal elements between ligand orbitals are assumed to be negligible, this matrix has nondiagonal elements only between the orthogonalized d-orbitals and the ligand group-orbitals of the same symmetry. The complete analytical solution of the monomer problem requires the diagonal elements of the Hamiltonian matrix, the overlap-integrals between the STO's and the nondiagonal Hamiltonian matrix elements. The first ones are virtually constant with respect to geometrical changes of the dimers and are taken to be the orbital energies of the atoms in the molecule. The overlap integrals can easily be represented in closed form[27] whereas the nondiagonal elements are approximated by:[25]

$$H_{mn}^{XY} = \frac{1}{2}\left(H_{mm}^{XX} + H_{nn}^{YY} + 2\overline{v}_{mn}^{XY}\right) \cdot S_{mn}^{XY} \qquad (13)$$

where *m,n* are any orbitals on the centers *X,Y*. H_{mm}^{XX} and H_{nn}^{YY} are the diagonal elements of the Hamiltonian matrix approximated by the orbital energies of atoms in the molecule. $\overline{v}_{mn}^{XY}$ is an angular-independent averaged potential of 2- and 3-centre Coulomb and exchange integrals $v_2, \overline{v}_3, \overline{v}_{xc}$ that are in good approximation proportional to S_{mn}^{XY}:[25]

$$\overline{v}_{mn}^{XY} = v_{mn}^{XY} / S_{mn}^{XY} = \left(v_2 + \overline{v}_3 + \overline{v}_{xc}\right) / S_{mn}^{XY} \qquad (14)$$

$\overline{v}_{mn}^{XY}$ is always negative and proportional to $1/R^2$ where *R* is the bonding distance between *X* and *Y*.[25] The resulting analytical approach, denoted as d-Hamiltonian,

has been proven to be sufficiently accurate for describing the antibonding MO's with predominantly d-character of transition metal monomers[25,26] representing therefore an adequate starting point for calculating H_{AB}. In order to derive sufficiently simple analytical formulas, ligand-ligand interactions as well as metal 4s- and 4p-orbitals were neglected in the monomer approach. Both are assumed to have negligible effects on magnetic coupling in ionic compounds, as well. Decomposing the dimer into two monomers *A* and *B*, the energy of the singly occupied monomer MO at centre *A* is given as[25]

$$\varepsilon_A^{\text{mono}} = H_{\text{dd}}^{AA} - \sum_i \left(2\bar{v}_{\text{id}}^{aA} + \frac{\left(\Delta_{\text{id}}^{aA} - 2\bar{v}_{\text{id}}^{aA}\right)^2}{4\Delta_{\text{id}}^{aA}} \right) \cdot S_{\text{id}}^{aA,2} \qquad (15)$$

with $\Delta_{\text{id}}^{aA} = H_{ii}^{aa} - H_{\text{dd}}^{AA}$ and an analogous expression for monomer *B*. The corresponding eigenfunction to ε_A^{mono}, *i.e.* the monomer MO, is given to first order in S_{id}^{aA} by

$$\psi_A^{mono} = N_A^{mono} \left(\left|\varphi_{\text{d}}^A\right\rangle - \sum_i \tau_{\text{id}}^{aA} S_{\text{id}}^{aA} \cdot \left|\varphi_i^a\right\rangle \right) \qquad (16)$$

where the coefficient $\tau_{\text{id}}^{aA} = \dfrac{\Delta_{\text{id}}^{aA} + 2\bar{v}_{\text{id}}^{aA}}{2\Delta_{\text{id}}^{aA}}$ is angular-independent and contains quantities that can be derived, *e.g.*, from spectroscopic data. Consequently, the whole angular dependence is contained in the overlap integrals S_{id}^{aA}. The overlap integral between these monomer MO's at centers *A* and *B* is calculated as

$$\begin{aligned} S_{AB}^{\text{mono}} &= \left\langle \psi_A^{\text{mono}} \middle| \psi_B^{\text{mono}} \right\rangle \\ &= N_A^{\text{mono}} N_B^{\text{mono}} \cdot \begin{pmatrix} S_{\text{dd'}}^{AB} - \sum_i \tau_{\text{d'}i}^{Bb} \cdot S_{i\text{d'}}^{bB} \cdot S_{\text{d}i}^{Ab} \\ -\sum_i \tau_{\text{d}i}^{Aa} \cdot S_{\text{id}}^{aA} \cdot S_{\text{d'}i}^{Ba} + \\ \sum_{i,j} \tau_{\text{d}i}^{Aa} \tau_{\text{d'}i}^{Bb} \cdot S_{\text{id}}^{aA} S_{i\text{d'}}^{bB} \cdot S_{ij}^{ab} \end{pmatrix} \end{aligned} \qquad (17)$$

where *i*, *j* run over all ligand orbitals on the magnetic centers *A* and *B*, respectively. In order to simplify this result, the following assumptions are made:

(i) ligand-ligand interactions are assumed to be negligible

$$H_{ij}^{aa} = H_{ij}^{aa} \cdot \delta_{ij};\ H_{ij}^{bb} = H_{ij}^{bb} \cdot \delta_{ij};$$
$$H_{kl}^{ab} = H_{lk}^{ba} = H_{kl}^{ab} \cdot \delta_{kl}$$
$$S_{ij}^{aa} = S_{ij}^{bb} = \delta_{ij};\ S_{kl}^{ab} = S_{lk}^{ba} = S_{kl}^{ab} \cdot \delta_{kl}$$

where *i,j* run over all ligand orbitals whereas *k,l* denote bridging orbitals

(ii) interactions between the metal and the terminal ligands at different monomers are neglected

(iii) for the special case of a symmetric complex further simplifications result

$$\begin{aligned} &H_{\text{dd}}^{AA} = H_{\text{dd}}^{BB} = H_{\text{dd}} \quad H_{ii}^{aa} = H_{ii}^{bb} = H_{ii} \\ &N_A^{\text{mono}} = N_B^{\text{mono}} = N^{\text{mono}} \\ &\tau_{\text{d}i}^{Aa} = \tau_{\text{d}i}^{Bb} = \tau_{\text{d}i};\ \tau_{\text{d}k}^{Ab} = \tau_{\text{d}k}^{Bb} = \tau_{\text{d}k} \\ &S_{\text{d}k}^{Aa} = S_{\text{d}k}^{Bb} = (\pm 1) S_{\text{d}k}^{Ab} = (\pm 1) S_{\text{d}k}^{Ba} \end{aligned} \qquad (18)$$

Thus, the site indices *A,B,a,b* can be omitted in these quantities. The factors (± 1) appears because the bridging group-orbitals for the two monomers may differ by sign, *e.g.* for a planar doubly bridged $\left[Cu_2X_2Y_4\right]^{n-}$ complex where the *xz*-plane is the molecular plane and *z* is the internuclear axis (Figure 1A) the following relations are fulfilled:

$$\left|\varphi_{\text{s}}^a\right\rangle = -\left|\varphi_{\text{s}}^b\right\rangle;\quad \left|\varphi_z^a\right\rangle = \left|\varphi_z^b\right\rangle;\quad \left|\varphi_x^a\right\rangle = -\left|\varphi_x^b\right\rangle \qquad (19)$$

where s, *z*, *x* denote s, p_z and p_x group orbitals. With these assumptions Eq. (17) reduces to

$$S_{AB}^{\text{mono}} = \left(N^{\text{mono}}\right)^2 \cdot \left(S_{\text{dd}}^{AB} - \sum_k \left(2\tau_{\text{d}k} - \tau_{\text{d}k}^2\right) \cdot S_{\text{kd}}^2 \cdot (\pm 1) \right) \qquad (20)$$

where the sign (± 1) depends on the bridging orbital *k*. Since $S_{AB}^{\text{mono}} < 0.05$, as will be shown below (Table 1), terms of order $\left(S_{AB}^{\text{mono}}\right)^n$ with $(n > 1)$ can be neglected. Inserting Eq. (20) together with Eq. (10) into Eq. (6) and neglecting higher order terms in $\left(S_{AB}^{\text{mono}}\right)^n$ and S_{dk}^{2n} $(n > 1)$ yields[28]

Table 1. Quantities required for calculating H_{AB} with Eq. (9) for three different bridging angles with the methods mon2, mon3

	82.5°		90°		110°	
	mon2	mon3	mon2	mon3	mon2	mon3
ε_A^{mono} / eV	−11.115	−10.541	−11.060	−10.500	−11.133	−10.583
H_{AB}^{mono} / eV	−0.111	−0.060	−0.135	−0.122	−0.003	−0.095
S_{AB}^{mono}	−0.014	−0.016	−0.0002	−0.0002	0.023	0.029
H_{AB} / cm^{-1}	−2156	−1865	−1108	−1004	2066	1720

$$H_{AB} = \overline{v}_{\mathrm{dd}}^{AB} \cdot S_{\mathrm{dd}}^{AB} - \sum_k \frac{\left(\Delta_{k\mathrm{d}} + 2\overline{v}_{k\mathrm{d}}\right)^2}{4\Delta_{k\mathrm{d}}} \cdot S_{\mathrm{d}k}^2 \cdot (\pm 1) \quad (21)$$

The first term, describing the direct d-d interaction, stems from the approximation for the nondiagonal element $H_{\mathrm{dd'}}^{AB}$ between atomic d-orbitals on different centers (*cf.* Eq. (13)). For ionic compounds as fluorides (see below) and oxides this simple expression for the transfer integral supplies results that can easily be interpreted and are in reasonable agreement with fully numerical calculations. Moreover, Eq. (21) can directly be improved by including further interactions, as metal 4s-, 4p-interactions, ligand-ligand interactions, *etc*.

However, if the energy differences between metal and ligand orbitals decrease or the nondiagonal elements are large, the perturbation calculation generally leads to poor results. In this case an alternative approach for the diagonalization will be used. The small contributions of the ligand s-orbitals can still be included as perturbations but will at first be neglected in the following discussion of the diagonalization procedure. The diagonalization of the Hamiltonian matrix is carried out in two different ways:

Bridging Ligand only Method. Assuming that in a symmetric complex the contributions from the terminal ligands cancel each other in the difference $\varepsilon_+ - \varepsilon_-$, Eq. (6), only the bridging ligands are explicitly included in the diagonalization procedure. The *m* diagonal-elements of the p-orbitals of the bridging ligands are averaged: $\overline{H}_{\mathrm{pp}} = \frac{1}{m}\sum_p H_{pp}$. This approximation is justified if the p-orbital energies are similar and energetically well separated from the orthogonalized metal d-orbital. The energy of the magnetic monomer orbital at site *A* and the corresponding eigenvector $\left|\psi_A^{\mathrm{mono}}\right\rangle$ are derived as

$$\varepsilon_A^{\mathrm{mono}} = \frac{1}{2}\left(\tilde{H}_{\mathrm{dd}}^{AA} + \overline{H}_{\mathrm{pp}}^{aa} + \sqrt{\left(\tilde{\Delta}_{\mathrm{pd}}^{aA}\right)^2 + 4\sum_p \left(\tilde{H}_{p\mathrm{d}}^{aA}\right)^2} \right) \quad (22)$$

$$\left|\psi_A^{\mathrm{mono}}\right\rangle = N_A^{\mathrm{mono}} \left(\tilde{\alpha}_{\mathrm{d}}^A \cdot \left|\tilde{\varphi}_{\mathrm{d}}^A\right\rangle + \sum_p \beta_p^a \left|\varphi_p^a\right\rangle \right) \quad (23)$$

where $\tilde{\Delta}_{\mathrm{pd}}^{aA} = \overline{H}_{\mathrm{pp}}^{aa} - \tilde{H}_{\mathrm{dd}}^{AA}$ and p runs over all bridging *p*-orbitals. $\tilde{H}_{\mathrm{dd}}^{AA} = \left\langle \tilde{\varphi}_{\mathrm{d}}^A \middle| H \middle| \tilde{\varphi}_{\mathrm{d}}^A \right\rangle$ is the energy of the ligand-orthogonalized d-orbital (Eq. (12)) and $\tilde{H}_{\mathrm{d}i}^{Aa} = \left\langle \tilde{\varphi}_{\mathrm{d}}^A \middle| H \middle| \varphi_i^a \right\rangle$ is the nondiagonal element with a ligand group p-orbital. The coefficients are obtained as

$$\tilde{\alpha}_{\mathrm{d}}^A = \frac{1}{2 \cdot \tilde{H}_{m\mathrm{d}}^{aA}} \left(-\tilde{\Delta}_{\mathrm{pd}}^{aA} + \sqrt{\left(\tilde{\Delta}_{\mathrm{pd}}^{aA}\right)^2 + 4 \cdot \sum_p \left(\tilde{H}_{p\mathrm{d}}^{aA}\right)^2} \right)$$

$$\beta_{\mathrm{p}}^a = \tilde{H}_{\mathrm{pd}}^{aA} / \tilde{H}_{m\mathrm{d}}^{aA}; \quad \beta_m^a = \tilde{H}_{m\mathrm{d}}^{aA} / \tilde{H}_{m\mathrm{d}}^{aA} = 1$$

where *m* is any of the ligand p-orbitals. Rewriting the eigenvector (23) in terms of the atomic d-orbital $\left|\varphi_{\mathrm{d}}^A\right\rangle$ gives

$$\begin{aligned} \left|\psi_A^{\mathrm{mono}}\right\rangle &= N_A^{\mathrm{mono}} \left(\alpha_{\mathrm{d}}^A \cdot \left|\varphi_{\mathrm{d}}^A\right\rangle + \sum_s \gamma_s^a \cdot \left|\varphi_s^a\right\rangle + \sum_p \gamma_p^a \left|\varphi_p^a\right\rangle \right) \\ &= N_A^{\mathrm{mono}} \left(\alpha_{\mathrm{d}}^A \cdot \left|\varphi_{\mathrm{d}}^A\right\rangle + \sum_i \gamma_i^a \cdot \left|\varphi_i^a\right\rangle \right) \end{aligned} \quad (24)$$

where $\alpha_{\mathrm{d}}^A = \tilde{\alpha}_{\mathrm{d}}^A \cdot N_{\mathrm{d}}^A$; $\gamma_{\mathrm{s}}^a = -\tilde{\alpha}_{\mathrm{d}}^A N_{\mathrm{d}}^A \cdot S_{\mathrm{sd}}^{aA}$; $\gamma_{\mathrm{p}}^a = \beta_{\mathrm{p}}^a - \tilde{\alpha}_{\mathrm{d}}^A N_{\mathrm{d}}^A \cdot S_{\mathrm{pd}}^{aA}$. The contribution from the s-orbital arises from the orthogonalization, whereas the small contribution from the diagonalization may be included by adding $-\left(\tilde{H}_{\mathrm{sd}}^{aA}\right)^2 / \Delta_{\mathrm{sd}}^{aA}$ to Eq. (24) and accordingly $-\tilde{H}_{\mathrm{sd}}^{aA} / \Delta_{\mathrm{sd}}^{aA} \cdot \tilde{\alpha}_{\mathrm{d}}^A$ to γ_{s}^a. The contributions of the terminal ligands, arising solely from the orthogonalization, are given as $\gamma_{\mathrm{p}}^a = -\tilde{\alpha}_{\mathrm{d}} \cdot N_{\mathrm{d}} \cdot S_{\mathrm{pd}}^{aA}$. Therefore, *i* in Eq. (24) runs over all ligand orbitals on the respective monomer.

Averaging Over All Ligands. If the terminal ligands of the monomers *A* and *B* are different, the cancellation of their contributions to the transfer integral cannot be expected. Therefore, the averaging procedure has to be extended to all ligand p-orbitals. Eqs. (22)–(24) can be applied in this case, as well, if the summations include the terminal ligands. This approximation again requires a clear energetic separation of metal and ligand orbitals. Both, the nondiagonal element $H_{AB}^{\mathrm{mono}} = \left\langle \psi_A^{\mathrm{mono}} \middle| H \middle| \psi_B^{\mathrm{mono}} \right\rangle$ and the overlap integral $S_{AB}^{\mathrm{mono}} = \left\langle \psi_A^{\mathrm{mono}} \middle| \psi_B^{\mathrm{mono}} \right\rangle$ can directly be calculated with either method. Using the relations (18) and $\alpha_{\mathrm{d}}^A = \alpha_{\mathrm{d}}^B = \alpha$ for a symmetric complex, these integrals are

$$\begin{aligned} H_{AB}^{\mathrm{mono}} &= \left\langle \psi_A^{\mathrm{mono}} \middle| H \middle| \psi_B^{\mathrm{mono}} \right\rangle \\ &= \left(N^{\mathrm{mono}}\right)^2 \left(\begin{array}{l} \alpha^2 \cdot H_{\mathrm{dd}}^{AB} + \\ \sum_k \left(2\alpha \cdot \gamma_k \cdot H_{\mathrm{d}k} + \gamma_k^2 \cdot H_{kk}\right)(\pm 1) \end{array} \right) \end{aligned} \quad (25)$$

$$\begin{aligned} S_{AB}^{\mathrm{mono}} &= \left\langle \psi_A^{\mathrm{mono}} \middle| \psi_B^{\mathrm{mono}} \right\rangle \\ &= \left(N^{\mathrm{mono}}\right)^2 \left(\begin{array}{l} \alpha^2 \cdot S_{\mathrm{dd}}^{AB} + \\ \sum_k \left(2\alpha \cdot \gamma_k \cdot S_{k\mathrm{d}} + \gamma_k^2\right)(\pm 1) \end{array} \right) \end{aligned} \quad (26)$$

with k being a bridging ligand orbital. $\varepsilon_A^{\text{mono}}$ is obtained as

$$\begin{aligned}\varepsilon_A^{\text{mono}} &= \left\langle \psi_A^{\text{mono}} \middle| H \middle| \psi_A^{\text{mono}} \right\rangle \\ &= \left(N_A^{\text{mono}}\right)^2 \left(\alpha^2 H_{\text{dd}}^{AA} + \sum_i \left(2a\gamma_i H_{\text{id}} + \gamma_i^2 H_{ii} \right) \right)\end{aligned} \tag{27}$$

with i running over all ligands on centre A. Inserting Eqs. (25–27) into Eq. (9) and neglecting terms od order $\left(S_{\text{dk}}\right)^n$, $n > 2$, yields

$$\begin{aligned}H_{AB} &= -\alpha^4 H_{\text{dd}}^{AA} \cdot S_{\text{dd}}^{AB} + \alpha^2 H_{\text{dd}}^{AB} \\ &- \sum_k \gamma_k \cdot \begin{pmatrix} \alpha^2 H_{\text{dd}}^{AA} \cdot \left(2\alpha S_{\text{dk}} + \gamma_k \right) \\ -2H_{\text{dk}}\alpha - H_{kk}\gamma_k \end{pmatrix} \cdot (\pm 1)\end{aligned} \tag{28}$$

This procedure avoids the problems of a perturbation calculation and, therefore, supplies better results than Eq. (21). In the case of strong ligand-ligand interactions it is necessary to orthogonalize explicitly the ligand orbitals among each other and to include their nondiagonal Hamiltonian matrix elements, as well. This may be required for ligands of the third or higher period or for molecular ligands where appropriate MO's interacting with the d-orbitals have to be constructed. In summary, the monomer approach presents the simplest way to calculate directly the transfer integral H_{AB}. Moreover, it enables the decomposition into single orbital contributions.

In this work the monomer approach is applied on symmetrical model systems. The extension to unsymmetrical and heteronuclear complexes is possible without difficulties and the results will be published elsewhere. Moreover, the monomer approach has turned out to work in principle also for strongly covalent complexes containing *e.g.* chlorine or sulphur ligands. However, the strong interactions of the ligand orbitals with the d-orbitals may cause significant energy differences between the ligand p-orbitals so that averaging and simple analytical diagonalization is impossible. This problem may be bypassed by directly constructing the dimer MO's $|\psi_+\rangle$ and $|\psi_-\rangle$.

B. Dimer Approach

The direct solution of the dimer problem, is analogous to the formalism developed for the monomers. The two dimer MO's belong to different irreducible representations of the symmetry group of the whole molecule. Thus, group-orbitals encompassing now orbitals from both centers A and B have to be constructed according to the respective symmetry (Figure 1(B)). With regard to this basis the Hamiltonian matrix splits into blocked matrices, which can be diagonalized separately by the methods discussed for the monomer approach. The respective highest eigenvalues (lowest binding energy) correspond to the energies of the magnetic orbitals ε_+, ε_-, Eq. (6), and diagonalization yields the eigenvalues

$$\varepsilon_\pm = \frac{1}{2}\left(\tilde{H}_{\text{dd}}^\pm + \bar{H}_{\text{pp}}^\pm + \sqrt{\left(\tilde{\Delta}_{\text{pd}}^\pm\right)^2 + 4 \cdot \sum_p \left(\tilde{H}_{p\text{d}}^\pm\right)^2} \right) \tag{29}$$

where $\tilde{\Delta}_{\text{pd}}^\pm = \bar{H}_{\text{pp}}^\pm - \tilde{H}_{\text{dd}}^\pm$. The s-orbitals may be included as perturbations again and the ligand-ligand interactions may be included if necessary in the same manner as described above. For an ionic system, as the Cu fluorides, it is also possible to derive $\varepsilon_\pm$ from a perturbation calculation, with the simple result

$$\varepsilon_\pm = \tilde{H}_{\text{dd}}^\pm - \sum_i \frac{\left(\tilde{H}_{i\text{d}}^\pm\right)^2}{\Delta_{i\text{d}}^\pm} \tag{30}$$

IV. APPLICATION

In a first series of applications the transfer integral is derived and analyzed for singly and doubly bridged Cu−F dimers. The results of the analytical approach are compared with fully numerical calculations in the local density approximation by the spin-polarized self-consistent charge Xα (SCC-Xα) method,[29,30] H_{AB} corresponds to half of the energy difference of the HOMO and LUMO orbitals in the spin restricted calculation, *cf.* Eq. (6).

A. The Monomer Approach for $[Cu_2F_6]^{2-}$

This ionic model dimer of symmetry $D_{2\text{h}}$ is assumed to have a Cu-F distance of 1.94 Å and an angle of 93° between Cu and the terminal ligands. The transfer integral will be calculated for bridging angles θ between 82.5° and 125°. The two CuF_4-monomers exhibit symmetry $C_{2\text{v}}$ (Figure 2) with magnetic orbitals transforming after the irreducible representation b_1 with predominantly Cu(d_{xz})-character if the *xz*-plane is defined as the molecular plane. According to the antibond-

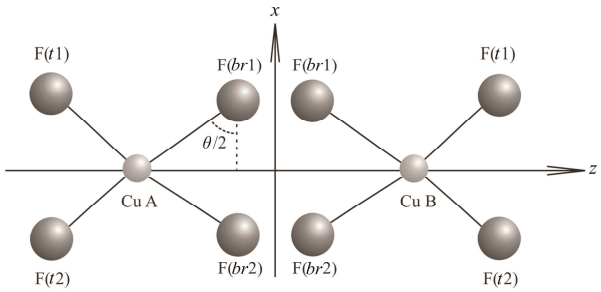

Figure 2. Decomposition of the $\left[Cu_2F_6\right]^{2-}$ complex into two monomers. *t* and *br* are terminal and bridging ligands, respectively.

ing character of this orbital the metal-ligand overlap matrix element is negative.

The analytical calculations are carried out in three different ways, *viz*. according to Eq. (21), denoted as mon1, and the two approaches for direct diagonalization, *i.e.* the bridging ligand only method (mon2) as well as the method averaging over all ligand energies (mon3) both using Eq. (28). The energy difference between the p-orbitals of terminal and bridging ligands before averaging is about 2.5 eV, and the least difference to the Cu(3d)-orbital about 3.5 eV. The resulting magnetic monomer orbitals exhibit large contributions (>0.90) from Cu(3d), contributions in the range 0.2–0.3 from the ligand p-orbitals and also small but nonnegligible ones from the ligand s-orbitals (0.05–0.10). Thus the spins are well localized at the transition metal.

The key quantities in Eqs. (25–27) required for the calculation of H_{AB}, Eq. (9), obtained with mon2 and mon3 are given in Table 1 for bridging angles of 82.5°, 90° and 110°.

Although H_{AB}^{mono}, Eq. (9), is not exactly proportional to the overlap integral S_{AB}^{mono} the data approximately reflect the empirically expected correlation between S_{AB}^{mono} and the transfer integral H_{AB}. Such a proportionality exists only for restricting to p-d interactions. Consequently, a more detailed physical interpretation may be supplied by analyzing separately the single orbital interactions given by Eq. (21) for mon1 and Eq. (28) for mon2 (*cf*. Table 2). The application of Eq. (28) with mon3 yields very similar results for this dimer and is therefore not listed in Table 2.

These results confirm the empirical Goodenough-Kanamori rules[4,5] predicting exact compensation of p-d interactions at 90°. However, due to direct d-d interactions and s-d contributions that are indeed not negligible, a vanishing transfer-integral is not obtained for a rectangular bridging angle, but the zero is shifted to somewhat larger angles (Figure 3).

Next, the transfer integrals H_{AB} for a series of different bridging angles θ, calculated with the three monomer methods (mon1-mon3) and Eq. (28) for mon2, are compared with the numerical values from the SCC-Xα calculation. The small differences between the columns of mon2 and Eq. (28) in Table 2 are due to simplifications arising from expanding Eq. (9) to arrive at Eq. (28) (see above). As shown in Figure 3, the numerical H_{AB} is an approximately linear function of θ vanishing at about 92°. The various analytical calculations exhibit a small uniform shift of the zero up to about 96° due to the neglect of ligand-ligand interactions as has been proven by model calculations. The slopes agree well with the numerical curve, except mon3 exhibiting an increasing slope above 110° instead of flattening. Especially with respect to the simplifying model assumptions, this must be considered as a satisfying result confirming the suitability of the analytical approach for investigating magneto-structural correlations.

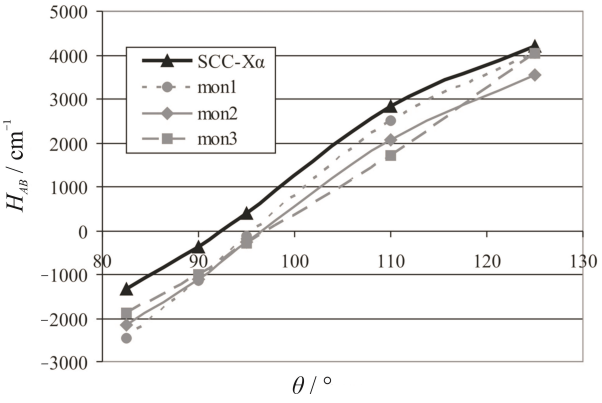

Figure 3. Comparison of the numerical H_{AB} (in cm^{-1}) from SCC-Xα with the three monomer approaches (mon1-mon3) for different bridging angles θ.

B. The Dimer Approach for a $[Cu_2F_6]^{2-}$ Complex

The energies of the two magnetic dimer orbitals are calculated according to Eq. (29). Again, the diagonalization is performed by averaging over all ligands (dim1), as well as with the bridging ligand only method (dim2) where also Eq. (30) is used. The results presented in Figure 4 show that analytical and numerical results for H_{AB} are again very similar with each other.

Consequently, this analysis demonstrates that at least for these symmetric double bridged dimers, both the monomer and the dimer approaches represent appropriate starting points for the calculation of H_{AB} and

Table 2. Contributions to H_{AB} (in cm^{-1}) from Eqs. (21) and (28) for different bridging angles. d-d: direct interaction between metals. *k*-d: interaction between metal d and a bridging orbital *k*

method	θ / °	d-d	s-d	*z*-d	*x*-d	H_{AB}
Eq. (21)	82.5	980	−1627	2814	−4627	−2460
	90	514	−1643	3717	−3717	−1129
	110	102	−1368	5051	−1284	2501
Eq. (28)	82.5	977	−1580	2637	−4307	−2282
	90	513	−1615	3486	−3486	−1089
	110	101	−1354	4799	−1219	2328

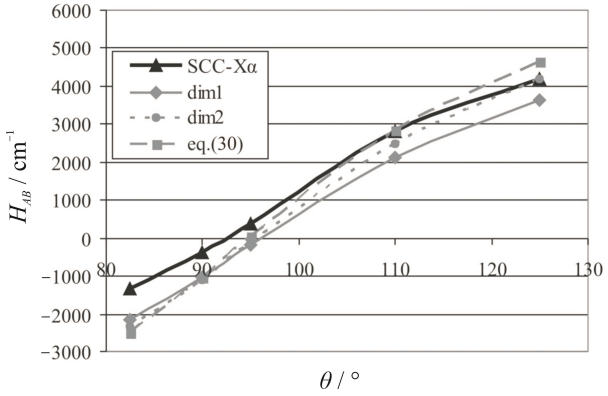

Figure 4. Comparison of the numerical H_{AB} (in cm^{-1}) from SCC-Xα with the two dimer approaches (dim1 and dim2) for different bridging angles θ.

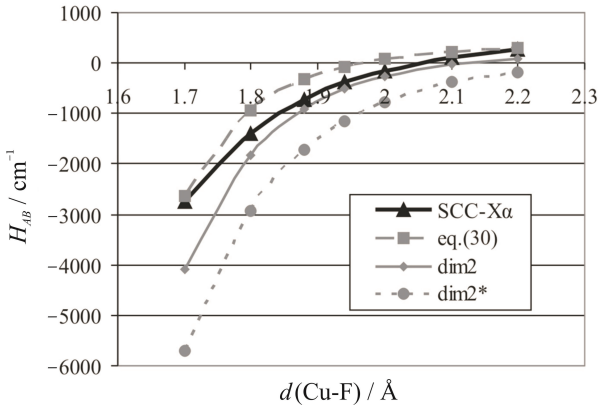

Figure 5. H_{AB} (in cm^{-1}) as a function of the bonding distance between Cu and the bridging ligands calculated with the dimer methods, dim2 and Eq. (30), and compared with the numerical values from SCC-Xα calculations. dim2* is the value without ligand-ligand interactions.

its geometrical dependencies. The larger slope of the transfer integral calculated with Eq. (30) arises from the different size of the matrix elements $\tilde{H}^{+}_{pd}$ and $\tilde{H}^{-}_{pd}$ of the symmetric and unsymmetrical magnetic orbitals, respectively, connected with small differences in the perturbation calculation. The contributions from orthogonalization and diagonalization for dim2 are given in Table 3.

At small and large angles the main contribution arises from diagonalization, while around 90–95° the contributions become comparable and compensate near 96°. In this case approximations for the diagonalization procedure obviously become crucial.

C. Variation of the Bonding Distance in $[Cu_2F_6]^{2-}$

In addition to the dependence of the transfer integral on the bridging angle, the distance dependence is investigated for the doubly bridged complex with a bridging angle fixed at 90°. In this case, the empirical rules for superexchange[4,5] predict ferromagnetic coupling. The bonding distance $d_{Cu\text{-}F}$ between Cu and the bridging ligands is varied between 1.7 and 2.2 Å whereas the distance to the terminal ligands is kept constant. At small distances the ligand-ligand interactions, even between terminal and bridging ligands, may become nonnegligible so that the dimer approach should be more suitable. Therefore, the interactions between the bridging orbitals as well as between bridging and terminal p_z orbitals are included. For diagonalization the bridging ligand only method, dim2, is being used since the p-orbital energies between terminal and bridging ligands may differ by several electron volts for small $d_{Cu\text{-}F}$. The results are shown in Figure 5 together with the values for neglecting ligand-ligand interactions and those obtained with Eq. (30).

As expected, ligand-ligand interactions are of crucial importance for small bonding distances. Due to these interactions the contributions from the terminal ligands are somewhat different for the symmetric and the antisymmetric magnetic orbital so that the compensation is not complete leading to significant deviations between dim2 and the numerical values at small bond-

Table 3. Contributions from orthogonalization (orth.) and diagonalization (dia) for dim2 (in cm^{-1})

θ / °	orth.	dia.	H_{AB}
82.5	−793	−1554	−2347
90	−586	−493	−1079
95	−363	264	−99
110	331	2162	2493
125	789	3416	4205

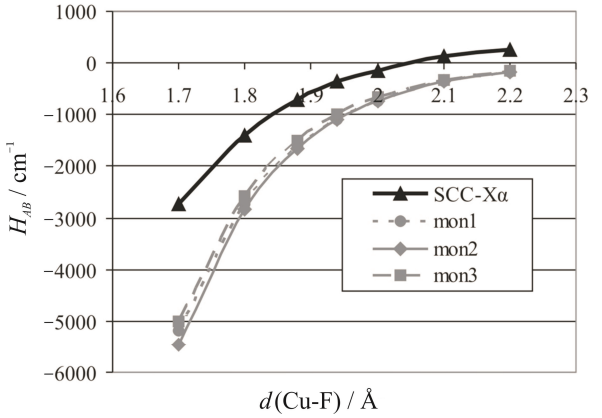

Figure 6. H_{AB} (in cm^{-1}) as a function of the bonding distance between Cu and the bridging ligands calculated with different monomer-methods, without ligand-ligand interactions, compared with the numerical values from SCC-Xα.

Table 4. d-d and s-d contributions (in cm^{-1}) to H_{AB} as a function of the bonding distance between Cu and the bridging ligands calculated with mon1

$d_{Cu\text{-}F}$ / Å	d-d	s-d
1.7	1939	−7318
1.8	1109	−3913
1.88	710	−2361
1.94	503	−1632
2	357	−1097
2.1	210	−575
2.2	120	−298

ing distances. However, since the ligand and metal orbitals are separated energetically by more than 4 eV a perturbation calculation is feasible for diagonalization. The results are depicted in Figure 5, denoted as Eq. (30), and are in reasonable accordance with the fully numerical calculation. The results of the monomer approaches without ligand-ligand interactions are shown in Figure 6.

As in the dim2* calculation, the transfer integral is overestimated for small bonding distances though qualitatively the correct behavior is reproduced. In order to understand the reasons for the deviations from the empirical 90° rule of ferromagnetic coupling, the contributions from the direct d-d and s-d interactions have to be analyzed (*cf.* Table 4). Since the values are taken from the mon1 calculations the p-d contributions cancel each other exactly. Consequently, the large value of the transfer integral for small bridging angles arises from the interaction with the ligand s-orbitals.

D. Singly Bridged $[Cu_2F_7]^{3-}$

This complex is treated only on the basis of the monomer approaches. Each monomer has symmetry C_{2v} with an assumed bonding distance of 1.94 Å. While the d-orbital contributing to the magnetic orbital of the planar, doubly bridged dimer orbitals was of pure d_{xz}-character, the magnetic orbital for nonlinear bridges (Figure 7) is a linear combination of three real d-orbitals (d_{yz}, d_{z^2}, $d_{x^2-y^2}$). Since the coefficients of the linear combination are not known a priori, each d-orbital has to be orthogonalized to the ligands separately. The resulting d-orbitals

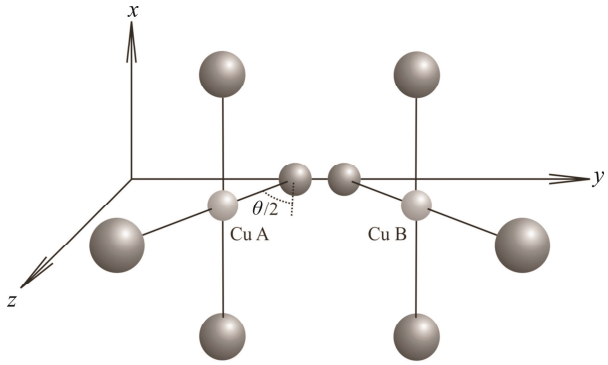

Figure 7. Singly bridged $[Cu_2F_7]^{3-}$ complex, decomposed into two monomers of symmetry C_{2v}.

are no longer orthogonal to each other, so that a second orthogonalization step is required. The final Hamiltonian matrix has nondiagonal elements in more than one column and row preventing an analytical diagonalization. For these reasons, the linear combination is estimated first: For a bridging angle of 180° the dimer is planar and only $d_{x^2-y^2}$ contributes to the magnetic monomer MO's if the molecule is placed in the *xy*-plane. The small contribution from d_{z^2} in the dimer arising from the slight distortion of the D_{4h} monomer-symmetry may safely be ignored. Assuming that the two magnetic centers interact only via their bridging ligand, the linear combination of the d-orbitals is in good approximation given by rotating the $d_{x^2-y^2}$-orbital into the monomer plane:

$$|d_{rot}\rangle = (\cos\alpha \cdot \sin\alpha)\cdot|d_{yz}\rangle + \left(\frac{1}{2}\sqrt{3}\sin^2\alpha\right)\cdot|d_{z^2}\rangle + \left(1-\frac{1}{2}\sin^2\alpha\right)\cdot|d_{x^2-y^2}\rangle \quad (31)$$

where $\alpha = (180° - \theta)/2$. Eq. (31) for the magnetic d-orbital enables treating the singly bridged dimer in the same manner as the doubly bridged one.

The analytical calculations are performed by the three monomer approaches mon1-mon3. The required quantities, Eqs. (25–27), are given in Table 5 for three bridging angles.

Again, the correlation between H_{AB} and S_{AB}^{mono} is not exactly linear for reasons discussed previously for

Table 5. Quantities required for calculating H_{AB} with Eq. (9) for three different bridging angles with the methods mon2, mon3

	80°		90°		120°	
	mon2	mon3	mon2	mon3	mon2	mon3
ε_A^{mono} / eV	−10.371	−9.850	−10.306	−9.791	−10.260	−9.732
H_{AB}^{mono} / eV	−0.094	−0.014	0.024	0.023	−0.030	−0.002
S_{AB}^{mono}	0.002	0.007	0.002	0.001	−0.006	−0.008
H_{AB} / cm^{-1}	555	424	321	298	−733	−653

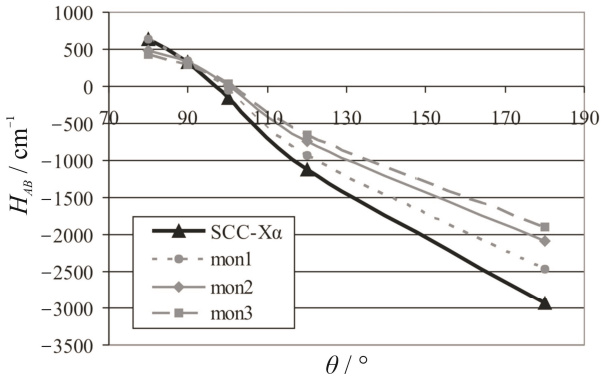

Figure 8. Comparison of H_{AB} (in cm^{-1}) from SCC-Xα and the three monomer approaches, respectively, for different bridging angles.

the doubly bridged dimer. The slope of the transfer integral with regard to increasing bridging angles is negative (Figure 8) due to the mirror plane (*xz*) between the monomers corresponding to the relations

$$\left|\varphi_s^a\right\rangle = \left|\varphi_s^b\right\rangle; \quad \left|\varphi_y^a\right\rangle = -\left|\varphi_y^b\right\rangle; \quad \left|\varphi_z^a\right\rangle = \left|\varphi_z^b\right\rangle \tag{32}$$

Accordingly, the overlap between the monomers via the bridging orbital $\left|\varphi_y^a\right\rangle$ parallel to the internuclear axis is negative, whereas for the doubly bridged complex this interaction, via $\left|\varphi_z\right\rangle$, is positive, *cf.* Eq. (19). A similar behavior is obtained for the other orbitals. As shown in Figure 8 analytical and fully numerical results compare very well.

V. CORRELATION BETWEEN H_{AB} AND J

Assuming that the variations with respect to geometry of both the ferromagnetic term, K_{AB}, and the effective Hubbard U with $U = U_{AA} - U_{AB}$, in Eq. (2) are small, the behavior of the coupling constant J as function of the geometry is dominated by the variations of H_{AB}. Accordingly, in exploring the geometry dependence J can be transformed into the parameterized form

$$J(fit) = C - 2 \cdot H_{AB}^2 \cdot f \tag{33}$$

where the parameters C and f are positive, geometry-independent constants. The applicability of Eq. (33) is tested on several different Cu-F dimers where both numerical and analytical transfer integrals are used. The results are compared with fully numerical calculations of J using the broken symmetry (bs) formalism.[8] In addition to the SCC-Xα method, the full potential local orbital (FPLO) code fplo7.00-28 (Ref. 31) is applied where the nonrelativistic mode and an exchange-only exchange-correlation potential has been used. Additionally, no Madelung potential is used in the FPLO-calculations.

A. Doubly Bridged $[Cu_2F_6]^{2-}$

In the first step the two-electron integrals in Eq. (2) are evaluated numerically for the $[Cu_2F_6]^{2-}$ complex using localized magnetic dimer orbitals constructed from the Kohn-Sham orbitals from the SCC-Xα calculations. The numerical calculations were performed with *Mathematica7*® enabling the direct calculation with localized magnetic dimer-orbitals. Alternatively, FORTRAN programs were developed. The results for K_{AB} and U as a function of the bridging angle vary within 10 % of their absolute values. Thus, H_{AB} is indeed the crucial parameter for exploring magneto-structural correlations. However, the numerical values of the two-electron integrals, especially U with about 9eV, are considerably too large. This is well known and may be traced back to the neglect of screening and rearrangement effects. On the other hand, the qualitative trend of U and K_{AB} being constant is not concerned, so that Eq. (33) is a good approximation.

In the next step, the geometrical variation of the coupling constant J is compared for:

(i) J(bs), from the broken symmetry calculations[8]

$$J(\mathrm{bs}) = \frac{E(S_{\max}) - E(S_{\min})}{S_{\max}^2 - S_{\min}^2} \tag{34}$$

where $S_{\max}$ and $S_{\min}$ are the spins of the high-spin and low-spin states, respectively, of the dimer, and $E(S)$ is the numerically obtained total energy of the spin state S.

(ii) J(fit), obtained by scaling the numerical H_{AB}' according to Eq. (33).

(iii) J(analyt), calculated with Eq. (33) and H_{AB} derived from the various analytical approaches.

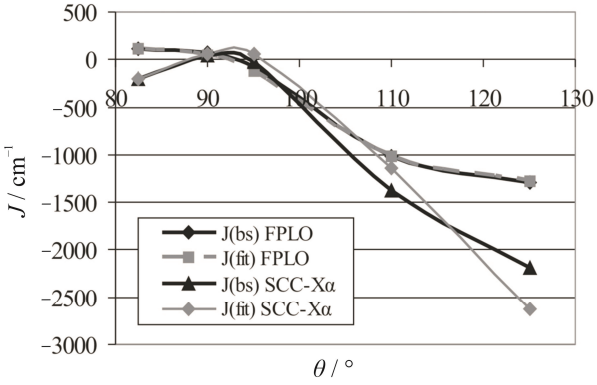

Figure 9. Comparison between J(bs) and the fitted J(fit) from SCC-Xα (C = 80 and f = 1/13000) and FPLO (C = 80 and f = 1/8500) calculations. (in cm^{-1})

Table 6. H_{AB}, J(bs), and J(fit) from FPLO where C = 110 and f = 1/7000 (in cm^{-1})

θ / °	H_{AB}	J(bs)	J(fit)
82.5	−46	110	109
90	475	67	46
95	889	−82	−116
110	1985	−1016	−1016
125	2203	−1292	−1277

Choosing C = 80 and f = 1/13000 in Eq. (33) for scaling the numerical H_{AB} from the SCC-Xα calculation (*cf.* Figure 3 or 4) yields coupling constants J(fit) in very good agreement with J(bs) as calculated by the SCC-Xα method in combination with the broken symmetry formalism (Figure 9) though some deviations occur at larger angles.

In order to assess these results and the validity of the assumptions analogous calculations were performed by FPLO. As shown in Table 6 and Figure 9, calculated and fitted coupling constants are virtually identical over the whole range of θ, confirming again that magneto-structural correlations are dominated by the variation of the transfer integral H_{AB}. The differences between SCC-Xα and FPLO may be traced back basically to the different basis sets.[29,31]

Applying Eq. (33) to the various monomer and dimer approaches (*cf.* Figures 3 and 4) yields the results displayed in Figure 10.

With regard to the simplifying model assumptions the analytical approaches reproduce the qualitative trend satisfactorily, and supply, thus, an easy way for interpreting the magnetic behavior.

B. $[Cu_2F_6]^{2-}$ with Varying Bonding Bistance

The behavior of the coupling constant as a function of the bonding distance between Cu and the bridging ligands, $d_{Cu\text{-}F}$, calculated with SCC-Xα can be well reproduced using Eq. (33) and the numerical transfer integrals (Figure 5 or 6). The coupling constant obtained with FPLO is again similar with the SCC-Xα one. The shift of the ferromagnetic region to smaller bonding

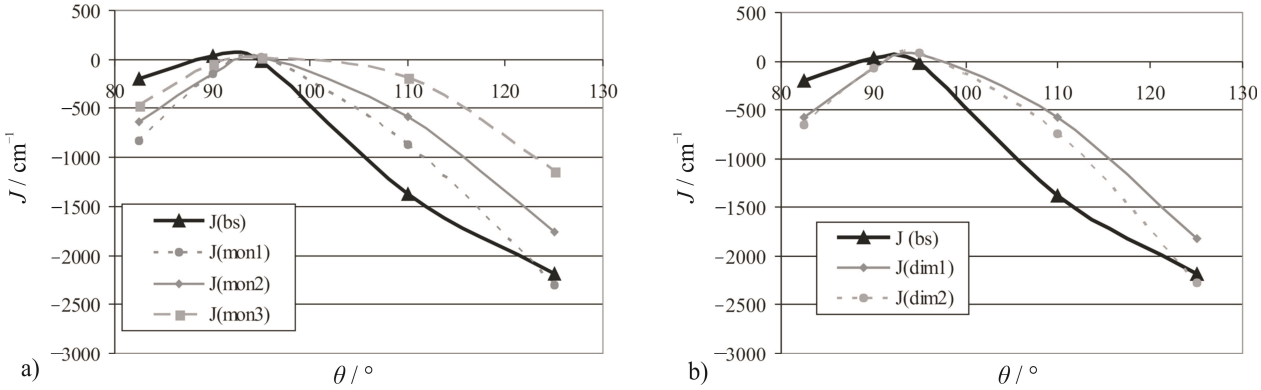

Figure 10. Comparison between J(bs) from SCC-Xα and J(analyt), in cm^{-1}, for H_{AB} taken from the (a) monomer (f = 1/7000 and C = 30) and (b) dimer approach (f = 1/15000 and C = 80).

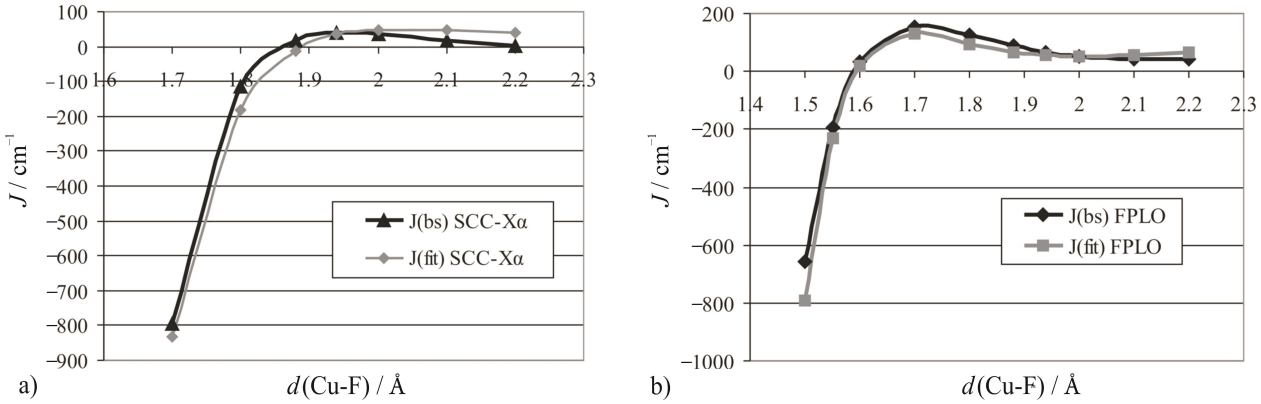

Figure 11. Comparison between J(bs) and the fitted J(fit) from (a) SCC-Xα, C = 50, f = 1/17000 , and (b) FPLO, C = 130, f = 1/6000 (in cm^{-1}).

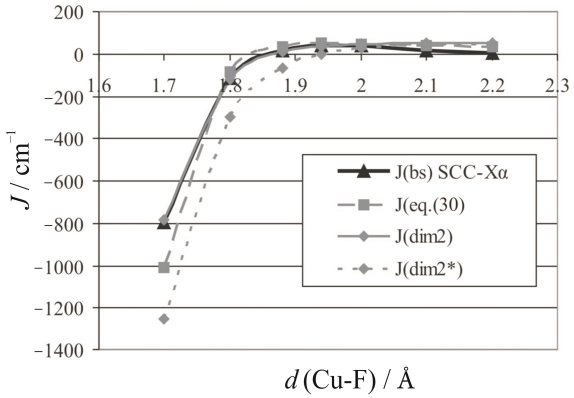

Figure 12. Comparison between J(bs) and J(analyt) for H_{AB} from the dimer approach dim2 (f = 1/40000, C = 50), the same approach without ligand-ligand interactions dim2* (f = 1/50000, C = 50) and the diagonalization with perturbation calculation Eq. (30) (f = 1/13000, C = 50).

distances is an effect of the omitted Madelung potential in the FPLO calculation. The results of both numerical methods are shown in Figure 11.

Again, there are small deviations between J(bs) and J(fit) in the SCC-Xα results which do not occur in the FPLO calculations. A very similar agreement of J(bs) and J(analyt) as for the numerical transfer integral from SCC-Xα is obtained with the analytical H_{AB} (*cf.* Figure 5). The results are depicted in Figure 12.

C. Singly Bridged $[Cu_2F_7]^{3-}$.

Finally, analogous calculations have been carried out for the singly bridged complex $[Cu_2F_7]^{3-}$. The results of the SCC-Xα and FPLO calculations are summarized in Figure 13.

The J(analyt) calculated with the analytical transfer integrals depicted in Figure 8 are shown in Figure 14. The agreement between the broken symmetry and the fitted results is again satisfactorily even for the ana-

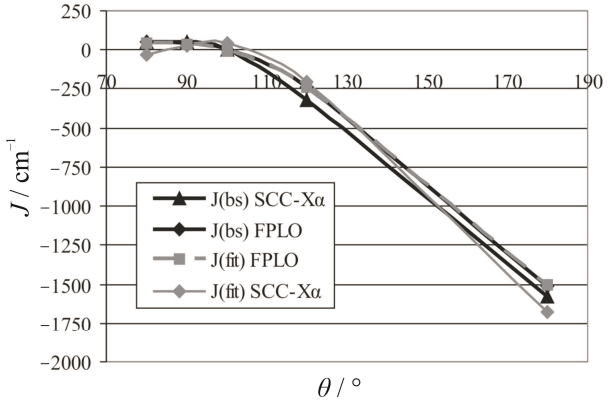

Figure 13. J(bs) and the fitted J(fit) from SCC-Xα (C = 50, f = 1/10000) and from FPLO (C = 80 and f = 1/8500) calculations.

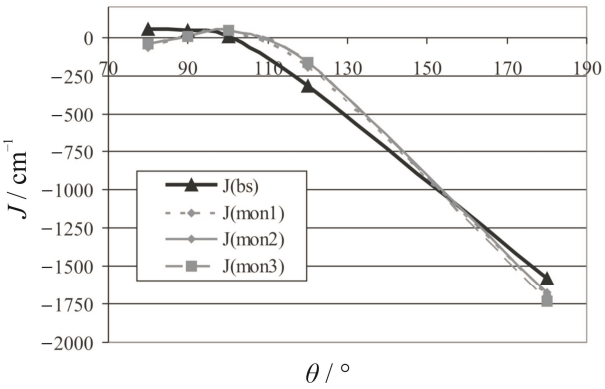

Figure 14. Comparison between J(bs) from SCC-Xα and J(analyt) for H_{AB} from the monomer approaches (mon1: f = 1/6000, C = 50; mon2: f = 1/5000, C = 50; mon3: f = 1/4000, C = 50).

lytical transfer integrals. However, for small bridging angles, the numerical calculation predicts a positive coupling constant while from the fitting procedure a negative J is obtained. This discrepancy might be attributed either to small geometry dependencies of the two-electron integrals or to additional higher order contributions. By contrast, this problem is not present in the FPLO results (Figure 13). Most likely, the discrepancy between J(bs) and J(fit) in SCC-Xα is an artifact of the small basis set. The good agreement of the coupling constants of both numerical codes calculated with the broken symmetry formalism confirms that most of the errors in the total energies of the two magnetic states cancel each other in the energy difference, Eq. (34).

VI. CONCLUSION

Analytical approaches, *viz*. various monomer and dimer approximations, were developed that enable the analytical calculation of transfer integrals H_{AB} and an estimate of the superexchange coupling constant. The monomer approaches supply compact and simple formulas especially suitable for ionic compounds, whereas the dimer approach additionally allows dealing with compounds exhibiting strong orbital interactions between transition metals and ligands. With regard to the simplifying model assumptions, the analytical results are in satisfactory agreement with fully numerical calculations on Cu-F model dimers. As commonly assumed and confirmed by numerical estimates, both the ferromagnetic contribution K_{AB} and the effective on-site interaction U can be taken as approximately constant. Since both cannot directly be calculated with sufficient reliability, two constant parameters were introduced. The applicability of the resulting parameterized formula for the superexchange coupling constant was tested by fitting numerically determined H_{AB} to numerical coupling constants

calculated with two different numerical methods. Especially the results from the numerical calculations with the FPLO code confirm that this is an excellent approximation. Therefore, the magneto-structural correlations in the superexchange coupled model compounds with fluorine ligands are fully described by the transfer integral. Similar results are obtained for copper-complexes with sulphur, chlorine or OH-ligands, as well, strongly interacting with the Cu-orbitals. The results for these covalent complexes will be published elsewhere. Consequently, if the magnetic behavior of a specific complex cannot be described as a function of the square of the transfer integral, *i.e.* with the suggested parameterized formula, this can be regarded as a hint that ligand spin polarization or other higher order terms, as ferromagnetic kinetic exchange, come into play. Such additional contributions occur if, *e.g.*, the magnetic orbitals are not clearly separated from the doubly occupied orbitals. Thus, the present approach may also be used as indicating such contributions.

As the main advantage, compared with other methods, these analytical approaches provide a simple scheme for estimating magnetic coupling constants on the basis of orbital interactions beyond simple empirical rules but without performing fully numerical calculations. Finally, it has to be emphasized that the applicability of this approach is not limited to symmetric dimers with one magnetic orbital per metal centre. Recent studies have shown that it is applicable as well to compounds with more than one unpaired electron per metal site (*e.g.* Fe-complexes). To this end, a generalized expression of Eq. (2)[23] and correspondingly of Eq. (33) has to be used. The formalism for calculating the single transfer integrals, however, is exactly the same as for the Cu-dimers. Moreover, especially the monomer approach can be extended to heteronuclear complexes. These results will be published soon.

Acknowledgements. This work has been financially supported by the Austrian Fonds zur Förderung der wissenschaftlichen Forschung (Project-No. P20503).

REFERENCES

1. R. D. Willett, D. Gatteschi, and O. Kahn, *Magneto-structural correlations in exchange coupled systems* (NATO ASI Series C **140**, Reidel, Dordrecht, The Netherlands, 1985).
2. A. Bencini and D. Gatteschi, *Electron paramagnetic resonance of exchange coupled systems*, Springer, New York, 1985.
3. A. P. Ginsberg, *Inorg, Chim. Acta Rev*. **5** (1971) 45.
4. J. B. Goodenough, *J. Phys. Chem. Sol.* **6** (1958) 287.
5. J. Kanamori, *J. Phys. Chem. Sol.* **10** (1959) 87.
6. P. W. Anderson, *Sol. St. Phys*. **14** (1963) 99.
7. R. G. Parr, W. Yang, *Density Functional Theory of Atoms and Molecules*, Oxford University Press Clarendon, New York, 1989.
8. L. Noodleman, *J. Chem. Phys.* **74** (1981) 5737.
9. D. J. Hodgson, *Progr. Inorg. Chem*. **19** (1975) 173.
10. E. I. Solomon, M. J. Baldwin, and M. D. Lowery, *Chem. Rev*. **92** (1992) 521.
11. J. G. Bednorz and K. Müller, *Z. Phys. B* **64** (1986) 189.
12. P. J. Hay, J. C. Thibeault, and R. Hoffmann, *J. Am. Chem. Soc.* **97** (1975) 4884.
13. P. de Loth, P. Cassoux, J. P. Daudey, and J. P. Malrieu, *J. Am. Chem. Soc*. **103** (1981) 4007.
14. L. Noodleman and E. R. Davidson, *Chem. Phys*. **74** (1986) 5737.
15. W. Geertsma, *Physica B* **164** (1990) 241.
16. A. E. Clark and E. R. Davidson, *J. Chem. Phys*. **115** (2001) 7382.
17. I. Mayer, *Chem. Phys. Lett*. **440** (2007) 357.
18. C. Herrmann, M. Reiher, and B. A. Hess, *J. Chem. Phys*. **122** (2005) 034102.
19. D. Seo, *J. Chem. Phys*. **127** (2007) 184103.
20. E. Ruiz, P. Alemany, S. Alvarez, and J. Cano, *J. Am. Chem. Soc*. **119** (1997) 1279.
21. O. Kahn, B. Briat, *J. Chem. Soc. Trans* 2 **72** (1976) 267.
22. O. Kahn and B. Briat, *J. Chem. Soc. Trans 2* **72** (1976) 1441.
23. O. Kahn, *Molecular Magnetism*, VCH, New York, 1993.
24. J. Appel, M. Grodzicki, and F. Paulsen, *Phys. Rev. B* **47** (1993) 2812.
25. S. Lebernegg, G. Amthauer, and M. Grodzicki, *J. Phys. B* **41** (2008) 035102.
26. S. Lebernegg, G. Amthauer, and M. Grodzicki, *J. Mol. Struct.* **924-926** (2009) 473.
27. M. Grodzicki, *Croat. Chem. Acta* **60** (1987) 263.
28. S. Lebernegg, Ph. D. Thesis, Salzburg (2010).
29. M. Grodzicki, *J. Phys. B* **13** (1980), 2683.
30. M. Grodzicki, Thesis of Habilitation, Hamburg (1985).
31. K. Koepernik and H. Eschrig, *Phys. Rev. B* **59** (1999) 1743.